Volcanic-tectonic seismicity at Stromboli (2005-2016)

Salvatore Gambino[1] and Antonio Scaltrito[1]

[1]*Istituto Nazionale di Geofisica e Vulcanologia, Sezione di Catania, P.zza Roma 2, 95123 Catania, Italy*

Submitted to: JVGR

Revised Version

(October, 2017)

Correspondence to:

Salvatore Gambino

Istituto Nazionale di Geofisica e Vulcanologia

Sezione di Catania

P.zza Roma 2, 95123 Catania, Italy

tel. number 39-95-7165800; fax number: 39-95-435801

e-mail: salvatore.gambino@ingv.it

Abstract

The seismicity of Stromboli comprises explosion-quakes, volcanic tremor and volcano-tectonic (VT) events. We applied the double-difference approach of Waldhauser and Ellsworth (2000) on 42 VT events recorded during 2005–2016 in order to improve their standard locations. This approach has allowed to cluster hypocentres in two seismogenic sectors (G1 and G2), respectively, located inside and south of Stromboli at depths of 3.5-6 and 10-12 km.

The seismicity belonging to G1 is located between the deep and intermediate magma storages of Stromboli and seems to precede the 2007 and 2014 effusive eruptions. This suggests that faulting episodes occur as a response to local stress linked to the pressurization of the magmatic system caused by magma ascent.

1.0 Introduction

High-precision earthquake locations are important for accurate seismological investigations and allow reconstructing the seismogenic structures, distinguishing between the fault planes in focal mechanisms and defining relationships between seismicity and volcanic processes (e.g. Alparone and Gambino, 2003; Lippitsch et al., 2005).

Stromboli is a strato-volcano, approximately 3 km high and rising 924 m above sea level (Fig. 1). It belongs to the Aeolian Islands archipelago, whose volcanism is expressed in seven islands and numerous seamounts making up an arc in the Tyrrhenian Sea, along the internal margin of the Appennine-Maghrebian chain. The volcano is located along a regional NE–SW structural trend and the edifice shows a quasi-bilateral symmetry on a NE-SW axis reflecting the main N41°E tectonic lineament controlling its formation (Bosman et al., 2009).

Typical, almost continuous, activity at Stromboli consists of intermittent explosions that occur at one or more of the summit craters every 10–20 minutes, with major explosions or paroxysms taking place with frequencies of 1–2 events per year (major explosions) or per century (paroxysms). Major paroxysms of the last century occurred on September 11, 1930 (Rittmann, 1931) and April 5, 2003

(Cesca et al., 2007). In addition, lava effusions, usually short-lived (days-weeks), are discharged from the summit craters or, more frequently, from vents opening up in the Sciara del Fuoco area (SdF), a deep depression in the NW flank of the volcano edifice (Barberi et al., 1993). During the last three decades, lava flowed into the SdF four times: in 1985-1986, 2002-2003, 2007, and most recently in 2014 (Bonaccorso et al., 2003; Calvari et al., 2005; Neri and Lanzafame, 2009; Rizzo et al., 2015).

Seismic monitoring of Stromboli has been performed continuously since 1985 (Falsaperla and Spampinato, 1999; Falsaperla et al., 2003). Stromboli comprises several typical signals, namely explosion-quakes (LP, VLP), volcanic tremor and volcano-tectonic (VT) earthquakes (e.g. Martini et al., 2007).

Moreover Stromboli area is also affected by very deep earthquakes (250-300 km) linked to the subduction beneath southern Italy (Neri et al., 2009).

In the last 30 years, only a few VT events have been recorded at Stromboli. The most powerful earthquakes occurred in November 1994 (Md=3.7, 7.7 Km depth), June 1999 (Md=3.2, 11.2 Km depth) and April 2006 (Md=3.3, 6.4 km depth) (Falsaperla et al., 1999; 2003; D'Auria et al., 2006).

Until 2002, locating VT seismicity in Stromboli area was almost impossible (owing to the small number of stations). The network was considerably improved after the paroxysm of April 2003, when a permanent network of 12 broadband digital seismic stations was deployed by INGV-OV in 2003 (Martini et al., 2007). However, the reliability of event locations is still limited since stations cover less than 3 km on the subaerial part of the volcano.

We considered a dataset comprising 42 VT events occurring from 2005 to 2016, whose strongest event was recorded on May 5, 2006 (M_L = 3.3). The locations for surveillance purposes show large mean errors of about 1.5-1.8 km ((http://www.ct.ingv.it/ufs/analisti/catalogolist.php).

We tried to make substantial improvements in earthquake location precision by using the double-difference relocation technique of Waldhauser and Ellsworth, (2000). Results are discussed as the relationships between tectonic activity and volcanism.

2.0 The network

Since 1977, continuous seismic monitoring activity on Aeolian Archipelago has been performed by a permanent seismic network made up of a few analog stations. Starting from the 80's, the network was extended by further seismic stations deployed over the entire Aeolian Archipelago equipped with short-period seismometers, having a natural frequency of 1 Hz. Since 2000's almost all stations were replaced by new digital 24-bit digitizers equipped with broadband (40s) three-component sensors.

The continuous seismic monitoring of the Stromboli island started in June 1985 with the first station (STR) equipped with a 1-Hz, vertical-component seismometer Geotech S-13 (Falsaperla et al., 2003). In 1993, STR was equipped with a three-component station and broadband records have been available since the mid-1990s also at two other seismic stations (TF1 and PL1), located in the western and southern part of the Stromboli island (Fig. 1). From September 1999 to March 2002, technical problems significantly reduced the possibility to record microseismicity, while a notable improvement of the monitoring system was introduced during the 2002–2003 eruptive crisis when a permanent network of 12 broadband digital seismic stations was installed by INGV–OV (Fig. 1, D'Auria et al., 2006). The stations are equipped with Guralp CMG 40T broadband sensors and signals are sampled at 50 Hz and data are transmitted by radio link to Osservatorio Vesuviano (INGV) in Naples and INGV monitoring centres in Catania and Rome.

Moreover, Udine University installed a seismic station in 1989 at Stromboli (Carniel et Jacop, 1996) and Florence University five seismic broadband sensors in 2003 (Ripepe et al., 2009).

Finally, Ocean Bottom Seismometers (OBS) installed during 2000-2001 in the Tyrrhenian Sea evidenced some micro-earthquakes that have been linked to the volcanic activity of Stromboli (Dahm et al., 2002; Sgroi et al., 2006).

3.0 Seismic data

The dataset used in this study comprises 42 earthquakes (Tab. 1), with magnitude $M_L \leq 3.3$, recorded from 2005 to 2016, whose locations (http://www.ct.ingv.it/ufs/analisti/catalogolist.php), performed for surveillance purposes, were obtained using the Hypoellipse code (Lahr, 1989) and a one-dimensional velocity crustal model (Tab. 2) derived, from Martinez-Arevalo et al., (2009) and Patanè et al., (2017).

This seismicity shows P and S phases with clear onsets and a spectral content between 1-10 Hz (Fig. 2); these features are similar to the 1999 Stromboli events described by Falsaperla and Spampinato (2003).

Figure 3 shows the cumulative strain release that was obtained as the square root of the seismic energy by using the Richter (1958) relationship:

$$\log E(erg) = 9.9 + 1.9M - 0.024\,M^2 \qquad (1)$$

The main episodes occurred in April-May 2006 (6 events with $M_{L\max}$ 3.3) and May-June 2014 (2 events with $M_{L\max} = 2.9$).

Earthquakes location (Fig. 4) evidences a seismicity in a deep range from 3 - 13 km; events located below Stromboli island are generally not deeper than 7 km.

4.0 Earthquake relocations and focal mechanisms

In order to acquire more precise relocations, we applied the double-difference earthquake algorithm of Waldhauser and Ellsworth (2000) and the HypoDD routine (Waldhauser, 2001) that takes advantage of the fact that if the hypocentral separation between two earthquakes is small enough compared to the event–station distance and the scale length of velocity heterogeneity, then the ray paths are similar along almost the entire length (Got et al., 1994). With this assumption, the differences in the travel times for two earthquakes recorded at the same station can be attributed to differences in their hypocentre spatial separation. In this way, errors due to inaccurately modeled velocity structure are minimized without the use of station corrections. This technique has been used in several studies (e.g. Bonforte et al., 2009; Alparone et al., 2013; Gambino et al., 2012) and produced sharp images of the studied fault structure.

During computation, HypoDD performs a reduction in the data as it groups the events into clusters of well-connected earthquakes and removes those considered outliers.

Although we started with an initial set of 42 events obtained from the first selection, our final data comprises 35 well-connected events. These events are connected through a network of links that consists of 2587 P and 500 S-wave phase pairs. The average number of links per event pair is 12, while the average offset between strongly linked events if about 2.8 km. We used the 1-D velocity model of table 2 and a Vp/Vs ratio of 1.73.

New locations show mean epicentral errors of 450 meters and 315 meters for focal depth.

In Fig. 5, a map and two sections of the seismicity located using HypoDD are shown; there is a significantly reduced scatter in locations, compared to figure 4, and two event groups are visible. The first (G1 in Fig. 5), made up of 15 events, roughly ENE-SSW oriented, 3.5-6 km deep, is located in the southern part of Stromboli; the second (G2, 13 events), 10-12 km deep, is 3-5 km south of Stromboli.

G1 includes the most powerful seismic events (M_L = 2.9 and M_L = 3.3) for the period which took place in April-December 2006 and from September 2010 to June 2014, (Fig. 3). G2 group includes events with M_L <2.5, occurring in particular during 2007 and 2008 (Fig. 3).

We computed fault plane solutions (FPSs) for the major and best-recorded earthquakes by using the first arrival P-wave polarities and the FPFIT code by Reasenberg and Oppenheimer (1985). We were able to determine only 3 FPSs, considering at least 10 first motion P-polarities (Fig. 5 and Tab. 3). The 2014 events show a prevalence of compressive mechanisms, while the 2006 main event is characterized by strike-slip.

5.0 Discussion and conclusions

Data from catalogues and seismic observations indicate a low occurrence rate of crustal VT earthquakes in the Stromboli area (e.g. Falsaperla and Spampinato, 1999; Falsaperla et al., 2003). In truth, until 2003, locations of VT proved very difficult to determine, leading to different interpretations of the same event (Falsaperla et al., 2003 and Mattia et al., 2008).

The first adequate locations are reported by D'Auria et al. (2006), who studied the VT events occurring in April-May 2006, positioning five events below the volcanic edifice at a depth of about 5÷6 km and also suggesting that they were triggered by a pressurization phase of the magmatic system.

We considered the period 2005-2016, characterized by 42 VT events that occurred mainly in the periods 2006-2008 and 2013-2014.

We obtained more precise locations by using the double-difference relocation technique of Waldhauser and Ellsworth (2000). This analysis reduced location errors from 1.5-2.0 km to 300-500 m, allowing to better investigate this seismicity and evidencing two main spatial groups, the first G1, 3.5-6.0 km deep with epicentres in south Stromboli and a second, G2, 10-12 km deep and located ca. 3-5 km south of the island.

We focused on the G1 group, observing that strain release and its occurrence (Fig. 3) increased during the months prior the two eruptions (2007 and 2014). The plausible triggering mechanism of these events may be a pressure increase in the plumbing system. The few focal mechanisms obtained show that the two 2014 events are compressive with NE-SW/NNE-SSW planes (according to the structural trend) while the 2006 events (D'Auria et al., 2006) seem to show strike-slip mechanisms E-W oriented. These differences may be linked to the fact that FPSs are very sensitive to event location and that D'Auria et al, (2006) obtained FPSs by using only the seismic stations of Stromboli, whereas we have also considered stations outside the island.

At Stromboli, zones of magma accumulation at different depths have been identified by geophysical and petrological data and reported in various recent papers (e.g. Bonaccorso et al., 2012; Di Traglia et al., 2015). The magma plumbing configuration (Fig. 6), is made up of:

1) a deep storage volume, refilled by Ca-basalts, which feeds towards surface the gas-rich, Low Porphyritic (LP) magma, erupted during the paroxysms, as inferred by petrology (Bertagnini et al., 2003; Francalanci et al., 2005; Di Carlo et al., 2006; Mètrich et al., 2010);
2) an intermediate storage, activated during the 2007 eruption and inferred by GPS and tilt data (Bonaccorso et al., 2008, 2009). This source, with a vertically elongated shape, had its centroid located at 2.6 km depth b.s.l., as was also recently confirmed by seismic tomography (Patanè et al 2017);
3) a shallow storage that is involved in all the surface and near-surface phenomena, including explosive activity, central and flank effusions, and non-eruptive (Chouet et al., 2003; James et al., 2006; Burton et al., 2007), with gas-poor, High Porphyritic (HP) magma (Métrich et al., 2005; Landi et al., 2006),

The G1 seismic group, 3.5-6.0 depth, is located (Fig. 6) between the upper part of the deep and the intermediate magma storage zone, suggesting the presence of seismogenic structures, between the two accumulation zones, which may be activated by significant magma ascent processes.

To conclude, showing new seismic locations inside the plumbing system model (Fig. 6), suggests that VT events, 3.5-6 km deep, may represent the crust fragile response to magma pressurization and ascent (from deep to intermediate storages) that preceded the 2007 and 2014 eruptions.

If future observations confirm our hypothesis, the occurrence of VT at these depths could represent a warning signal of ongoing effusive activity at Stromboli.

Acknowledgements

We want to thank Thomas Braun and an anonymous referee for their comments leading to substantial improvements of the manuscript. Thanks to S. Conway for correcting and improving the English of the paper.

References

Alparone, S., Gambino, S., 2003. High precision locations of multiplets on south-eastern flank of Mt. Etna (Italy): reconstruction of fault plane geometry. Phys. Earth Plan. Int. 135, 281-289.

Alparone, S., Cocina, O., Gambino, S., Mostaccio, A., Spampinato, S., Tuvè, T., Ursino, A., 2013. Seismological features of the Pernicana–Provenzana Fault System and implications for the dynamics of northeastern flank of the volcano. J. Volcanol. Geotherm. Res. http://dx.doi.org/10.1016/j.jvolgeores.2012.03.010.

Barberi, F., Rosi, M., Sodi, A., 1993. Volcanic hazard assessment at Stromboli based on review of historical data. Acta Vulcanologica 3, 173–187.

Bertagnini, A., Métrich, N., Landi, P., Rosi, M., 2003. Stromboli volcano (Aeolian Archipelago, Italy): an open window on the deep-feeding system of a steady state basaltic volcano. J. Geophys. Res. 108 (B7), 2336. http://dx.doi.org/10.1029/2002JB002146.

Bonaccorso, A., Calvari, S., Garfì, G., Lodato, L., Patané, D., 2003. December 2002 flank failure and tsunami at Stromboli volcano inferred by volcanological and geophysical observations. Geophys. Res. Lett. 30 (18), 1941–1944.

Bonaccorso, A., Gambino, S., Guglielmino, F., Mattia, M., Puglisi, G., Boschi, E., 2008. Stromboli 2007 eruption: deflation modeling to infer shallow-intermediate plumbing system. Geophys. Res. Lett. 35, L06311. http://dx.doi.org/10.1029/2007GL032921.

Bonaccorso, A., Bonforte, A., Gambino, S., Mattia, M., Puglisi, G., 2009. Insight on recent Stromboli eruption inferred from terrestrial and satellite deformation measurements. J. Volcanol. Geotherm. Res. 182, 172–181.

Bonaccorso, A., Calvari, S., Linde, A., Sacks, S. & Boschi, E., 2012. Dynamics of the shallow plumbing system investigated from borehole strainmeters and cameras during the 15 March, 2007 Vulcanian paroxysm at Stromboli volcano. Earth Planet. Sci. Let. 357, 249–256.

Bonforte, A., Gambino, S., Neri, M., 2009. Intrusion of eccentric dikes: The case of the 2001 eruption and its role in the dynamics of Mt. Etna volcano. Tectonophysics 471, 78-86.

Bosman A, Chiocci FL, Romagnoli C. (2009). Morpho-structural setting of Stromboli volcano revealed by high-resolution bathymetry and backscatter data of its submarine portions. Bull Volcanol., 71, 1007–1019. doi: 10.1007/s00445-009-0279-5.

Burton, M.R., Allard, P., Murè, F., La Spina, A., 2007. Magmatic gas composition reveals the source depth of slug-driven Stromboli an explosive activity. Science 317, 227–230.

Calvari, S., Spampinato, L., Lodato, L., Harris, A.J.L., Patrick, M.R., Dehn, J., Burton, M.R., Andronico, D., 2005. Chronology and complex volcanic processes during the 2002–2003 flank eruption at Stromboli volcano (Italy) reconstructed from direct observations and surveys with an handheld thermal camera. J. Geophys. Res. 110, B02201. http://dx.doi.org/10.1029/2004JB003129.

Carniel, R., Iacop F. (1996), Spectral precursors of paroxysmal phases of Stromboli. Ann. Geof., 39, 2, 327-359.

Cesca, S., Braun, T., Tessmer, E. and T. Dahm (2007), Modelling of the April 5, 2003, Stromboli (Italy) paroxysmal eruption from the inversion of broadband seismic data, Earth Plan. Sci. Lett., 261, 164-178.

Chouet, B., P. Dawson, T. Ohminato, M. Martini, G. Saccorotti, F. Giudicepietro, G. De Luca, G. Milana, and R. Scarpa., 2003. Source mechanisms of explosions at Stromboli Volcano, Italy, determined from moment-tensor inversions of very-long-period data, J. Geophys. Res., 108(B1), 2019, doi:10.1029/2002JB001919.

Dahm, T., M. Thorwart, E. Flueh, T. Braun, R. Herber, P. Favali, L. Beranzoli, G. D'Anna, F. Frugoni, and G. Smirglio (2002). Ocean bottom seismological instruments deployed in the Tyrrhenian Sea, EOS Trans. 83, 309, 314.

D'Auria, L., Giudicepietro, F., Martini, M., Orazi, M., 2006. The April-May 2006 Volcano-Tectonic Events at Stromboli Volcano (Southern Italy) and their Relation with the Magmatic System. Earth Prints Repository open archives (http://hdl.handle.net/2122/1506).

Di Carlo, I., Pichavant, M., Rotolo, S.G., Scaillet, B., 2006. Experimental crystallization of a high-Karcbasalt: the golden pumice, Stromboli volcano (Italy). J. Petrol. 47,1317–1343.

Di Traglia, F., Battaglia, M., Nolesini, T., Lagomarsino, D., Casagli, N., 2015. Shifts in the eruptive styles at Stromboli in 2010–2014 revealed by ground-based InSAR data. Sci. Rep. 5:13569. http://dx.doi.org/10.1038/srep13569.

Falsaperla, S., Spampinato, S., 1999. Tectonic seismicity at Stromboli volcano (Italy) from historical data and seismic records. Earth Planet. Sci. Lett. 173, 425–437.

Falsaperla, S., Alparone, S., Spampinato, S., 2003. Seismic features of the June 1999 tectonic swarm in the Stromboli volcano region, Italy. J. Volcanol. Geotherm. Res. 125, 121–136.

Finizola, A., Sortino, F., Lenat, J.F., Valenza, M., 2002. Fluid circulation at Stromboli volcano (Aeolian Islands, Italy) from self-potential and CO2 surveys. J. Volcanol. Geoth. Res.116, 1–18.

Francalanci, L., Davies, G.R., Lustenhouwer, W., Tommasini, S., Mason, P.R.D., Conticelli, S., 2005. Intra-Grain Sr isotope evidence for crystal recycling and multiple magma reservoirs in the recent activity of Stromboli volcano, Southern Italy. J. Petrol. 46 (10), 1997–2021. doi:10.1093/petrology/egi045.

Gambino, S., Milluzzo, V., Scaltrito, A., Scarfì, L., 2012. Relocation and focal mechanisms of earthquakes in the south-central sector of the Aeolian Archipelago: new structural and volcanological insights. Tectonophysics 524–525, 108–115.

Got, J., Fréchet, J., Klein, F.W., 1994. Deep fault plane geometry inferred from multiplet relative relocation beneath the south flank of Kilauea. J. Geophys. Res. 99, 15375-15386.

James, M.R., Lane, S.L., Chouet, B.A., 2006. Gas slug ascent through changes in conduit diameter: laboratory insights into a volcano-seismic source process in low-viscosity magmas. J. Geophys. Res. 111, B05201. http://dx.doi.org/ 10.1029/2005JB003718.

Lahr, J.C., 1989. HYPOELLIPSE/VERSION 2.0: A computer program for determining local earthquake hypocentral parameters, magnitude, and first motion pattern. U.S. Geol. Survey, Open-File Report 89/116, 81 pp.

Landi, P., Francalanci, L., Pompilio, M., Rosi, M., Corsaro, R.A., Petrone, C.M., Nardini, I., Miraglia, L., 2006. The December 2002–July 2003 effusive event at Stromboli volcano, Italy: insights into the shallow plumbing system by petrochemical studies. J. Volcanol. Geotherm. Res. 155, 263–284.

Lippitsch, R., White, R., Soosalu, H., 2005. Precise hypocenter relocation of microearthquakes in a high- temperature geothermal field: the Torfajökull central volcano, Iceland. Geophys. J. Int. 160, 371-388.

Martinez-Arevalo, C., C. Musumeci, and D. Patane` (2009), Evidence of a partial melt zone beneath Stromboli volcano (Italy) from inversion of teleseismic receiver functions, Terra Nova, 21, 386-392.

Martini, M., Giudicepietro, F., D'Auria, L., Esposito, A.M., Caputo, T., Curciotti, R., De Cesare, W., Orazi, M., Scarpato, G., Caputo, A., Peluso, R., Ricciolino, P., Linde, A., Sacks, S., 2007. Seismological monitoring of the February 2007 effusive eruption of the Stromboli volcano, Ann. Geophys. 50, 775–788.

Mattia M., Aloisi M., Di Grazia G., Gambino S., Palano M., Bruno V., 2008. Geophysical investigations of the plumbing system of Stromboli volcano (Aeolian Islands, Italy). J Volcanol Geotherm Res 176:529–540.

Métrich, N., Bertagnini, A., Landi, P., Rosi, M., Belhadj, O., 2005. Triggering mechanism at the origin of paroxysms at Stromboli (Aeolian Archipelago, Italy): the 5 April, 2003 eruption. Geophys. Res. Lett. 32, L10305. http://dx.doi.org/10.1029/2004GL022257.

Métrich, N., A. Bertagnini, and A. Di Muro 2010. Conditions of magma storage, degassing and ascent at Stromboli: New insights into the volcano plumbing system with interferences on the eruptive dynamics, J. Petrol., 51, 603–626, doi:10.1093/petrology/egp083.

Neri, M., Lanzafame, G., 2009. Structural features of the 2007 Stromboli eruption. J. Volcanol. Geotherm. Res. 182, 137–144. http://dx.doi.org/10.1016/ j.jvolgeores.2008.07.021.

Neri, G., Orecchio, B., Totaro, C., Falcone, G., Presti, D., (2009) Subduction beneath Southern Italy close the ending: results from seismic tomography. Seism. Res. Lett., 80, 1, 63-69.Patanè, D., G. Barberi, P. De Gori, O. Cocina, L. Zuccarello, A. Garcia-Yeguas, M. Castellano, A. D'Alessandro, and T. Sgroi (2017), The shallow magma chamber of Stromboli volcano (Italy), Geophys. Res. Lett., 44, doi:10.1002/2017GL073008.

Reasenberg, P., Oppenheimer, D., 1985. FPFIT, FPPLOT and FPPAGE: FORTRAN computer programs for calculating and displaying fault plane solutions. U.S. Geol. Surv. Open File Rep. 85/739, 109 pp.Richter, C.F. (1958). Elementary Seismology. Freeman, San Francisco.

Ripepe, M., D. Delle Donne, G. Lacanna, E. Marchetti, and G. Ulivieri (2009), The onset of the 2007 Stromboli effusive eruption recorded by an integrated geophysical network, J. Volcanol. Geotherm. Res., 182, 131–136, doi:10.1016/j.jvolgeores.2009.02.011.

Rittmann A. (1931) Der ausbruch des Stromboli am 11 September 1930. Zeitschift für vulkanologie 14:47–77.

Rizzo, A. L., Federico, C., Inguaggiato, S., Sollami, A., Tantillo, M., Vita, F., Bellomo, S., Longo, M., Grassa, F., Liuzzo, M., 2015. The 2014 effusive eruption at Stromboli volcano (Italy): Inferences from soil CO2 flux and 3He/4He ratio in thermal waters. Geophys. Res. Lett. 42, 2235–2243. http://dx.doi.org/10.1002/2014GL062955.

Sgroi, T., T. Braun, T. Dahm, and F. Frugoni (2006), An improved seismi-city picture of the Southern Tyrrhenian area by the use of OBS and land-based networks: The TYDE experiment, Ann. Geophys., 49, 801 – 817.

Tibaldi, A., Corazzato, C., Marani, M., Gamberi, F., 2009. Subaerial-submarine evidence of structures feeding magma to Stromboli Volcano, Italy, and relations with edifice flank failure and creep. Tectonophysics 469 (1–4), 112–136.

Waldhauser, F., Ellsworth, W.L., 2000. A double-difference earthquake location algorithm: Method and application to the northern Hayward fault. Bull. Seism. Soc. Am. 90, 1353-1368.

Waldhauser, F., 2001. HypoDD: A computer program to compute double-difference earthquake locations. U.S. Geol. Surv. Open-File Report 01-113.

Captions

Fig. 1 – Aeolian Archipelago structural map and seismic network. Structural features are redraw from Finizola et al., (2002) and Tibaldi et al., (2009).

Fig. 2 – Seismograms and spectra of a VT (05/05/2006 H=20:49) and an explosion-quake (11/09/2011 H=20:18).

Fig. 3 - Strain release of the entire seismic dataset and of G1 and G2 groups (see their location on Figure 5).

Fig. 4 - Epicentral map of the 2005-2016 earthquakes performed for surveillance purposes. Vertical scale is slightly amplified.

Fig. 5 - Map and vertical cross sections of the seismicity relocated using HypoDD and focal mechanisms. Vertical scale is slightly amplified.

Fig. 6- Final interpretation scheme. Schematic section of the Stromboli multiple-zone storage plumbing system, inferred by integrating previous geophysical, geochemical and petrological results together with the relocated seismicity.

Tables

Tab. 1 List of the VT-events reporting magnitude and standard locations.

Tab. 2 Stromboli velocity model.

Tab. 3 Fault plane solutions.

Table 1

Layer	Vp (km/s)	Top (km b.s.l.)	Bottom (km b.s.l.)	Vp/Vs
1	2.8	0.0	0.4	1.73
2	3.5	0.4	0.8	1.73
3	4.8	0.8	3.8	1.73
4	5.2	3.8	6.8	1.73
5	5.7	6.8	9.8	1.73
6	5.3	9.8	12.8	1.73
7	4.9	12.8	15.8	1.73
8	6.5	15.8	18.8	1.73
9	7.9	18.8	30.0	1.73

Table 2

N	Time	Ml	Latitude N	Longitude E	Depth (km) b.s.l.
1	**2006-04-10 12:28**	**1.5**	**38.816**	**15.198**	**1.3**
2	**2006-04-18 19.31**	**3.2**	**38.811**	**15.207**	**4.5**
3	**2006-05-05 20.49**	**3.3**	**38.785**	**15.206**	**7.2**
4	**2006-05-06 21.09**	**2.0**	**38.766**	**15.204**	**6.2**
5	**2006-05-22 19.21**	**2.5**	**38.799**	**15.231**	**5.7**
6	**2006-06-05 15.53**	**2.1**	**38.714**	**15.182**	**6.1**
7	**2006-07-04 04.07**	**1.8**	**38.81**	**15.191**	**5.9**
8	**2006-07-04 04.37**	**1.6**	**38.801**	**15.192**	**5.2**
9	**2006-07-04 06.54**	**1.8**	**38.794**	**15.217**	**2.6**
10	**2006-07-21 05.11**	**2.3**	**38.784**	**15.222**	**5.1**
11	**2006-07-21 12.59**	**2.1**	**38.766**	**15.257**	**8.0**
12	**2006-09-08 00.10**	**2.2**	**38.789**	**15.208**	**3.4**
13	**2006-10-23 13.57**	**1.5**	**38.81**	**15.199**	**2.4**
14	**2006-12-11 22.01**	**2.5**	**38.791**	**15.212**	**4.1**
15	**2007-07-01 10.29**	**1.8**	**38.74**	**15.187**	**10.1**
16	**2007-07-01 12.09**	**2.0**	**38.734**	**15.162**	**7.9**
17	**2007-07-03 00.23**	**2.2**	**38.745**	**15.178**	**9.4**
18	**2007-07-25 12.24**	**1.9**	**38.809**	**15.256**	**0.3**
19	**2008-05-16 17.28**	**2.2**	**38.723**	**15.178**	**8.1**
20	**2008-06-09 05.26**	**2.0**	**38.713**	**15.25**	**7.3**
21	**2008-07-01 09.39**	**2.0**	**38.754**	**15.194**	**12.2**
22	**2008-07-06 05.30**	**2.2**	**38.738**	**15.195**	**10.3**
23	**2008-07-06 07.30**	**1.9**	**38.741**	**15.186**	**8.5**
24	**2008-07-06 23.59**	**2.0**	**38.752**	**15.165**	**9.5**
25	**2008-07-10 04.49**	**2.0**	**38.749**	**15.162**	**10.0**
26	**2008-07-17 02.28**	**2.2**	**38.741**	**15.184**	**10.0**
27	**2008-07-29 15.58**	**2.1**	**38.729**	**15.198**	**9.6**
28	**2008-08-02 19.10**	**1.9**	**38.742**	**15.15**	**6.1**
29	**2009-05-06 17.21**	**1.6**	**38.724**	**15.224**	**10.1**
30	**2010-09-25 22.15**	**2.3**	**38.774**	**15.215**	**4.4**
31	**2011-01-19 14.45**	**1.3**	**38.758**	**15.191**	**9.7**
32	**2011-03-13 21.10**	**2.3**	**38.782**	**15.221**	**2.8**
33	**2011-12-16 12.49**	**2.2**	**38.736**	**15.232**	**11.9**
34	**2012-09-01 02.47**	**2.5**	**38.759**	**15.244**	**5.2**
35	**2012-11-05 12.10**	**1.9**	**38.761**	**15.227**	**6.0**
36	**2013-07-17 12.36**	**2.1**	**38.773**	**15.198**	**0.7**
37	**2013-07-20 02.28**	**1.2**	**38.778**	**15.216**	**3.3**
38	**2013-07-20 10.16**	**1.3**	**38.789**	**15.213**	**1.7**
39	**2013-09-24 02.57**	**1.8**	**38.735**	**15.205**	**13.2**
40	**2013-10-14 15.16**	**2.2**	**38.757**	**15.259**	**6.0**
41	**2014-05-26 00.41**	**2.9**	**38.791**	**15.223**	**5.4**
42	**2014-06-16 06.21**	**2.3**	**38.78**	**15.239**	**6.9**

Table 3

N	DATE	O.T.	LAT	LON	M_L	Z [km]	Strike	Dip	Rake
1	05/05/2006	20:49:24	38.7743	15.2105	3.3	6.222	80	40	170
2	26/05/2014	00:41:54	38.7851	15.2129	2.6	4.281	40	40	110
3	16/06/2014	06:21:28	38.7776	15.2126	2.3	5.812	220	65	60

Fig. 1

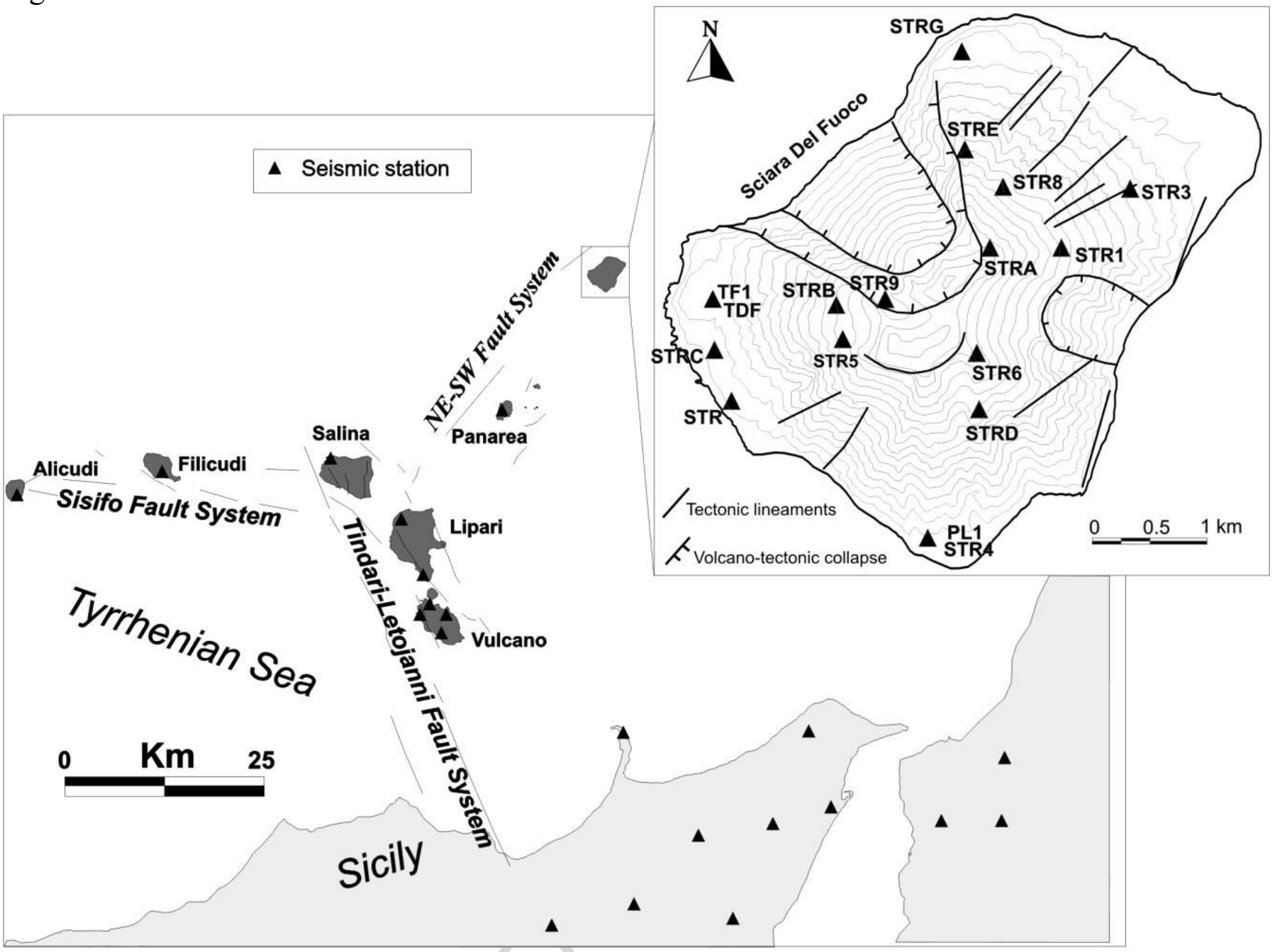
Seismic station
NE-SW Fault System
Salina
Panarea
Alicudi
Filicudi
Sisifo Fault System
Lipari
Vulcano
Tindari-Letojanni Fault System
Tyrrhenian Sea
0 Km 25
Sicily
N
STRG
Sciara Del Fuoco
STRE
STR8
STR3
STRA
STR1
TF1
TDF
STRB
STR9
STRC
STR5
STR6
STR
STRD
Tectonic lineaments
Volcano-tectonic collapse
PL1
STR4
0 0.5 1 km

Fig. 2

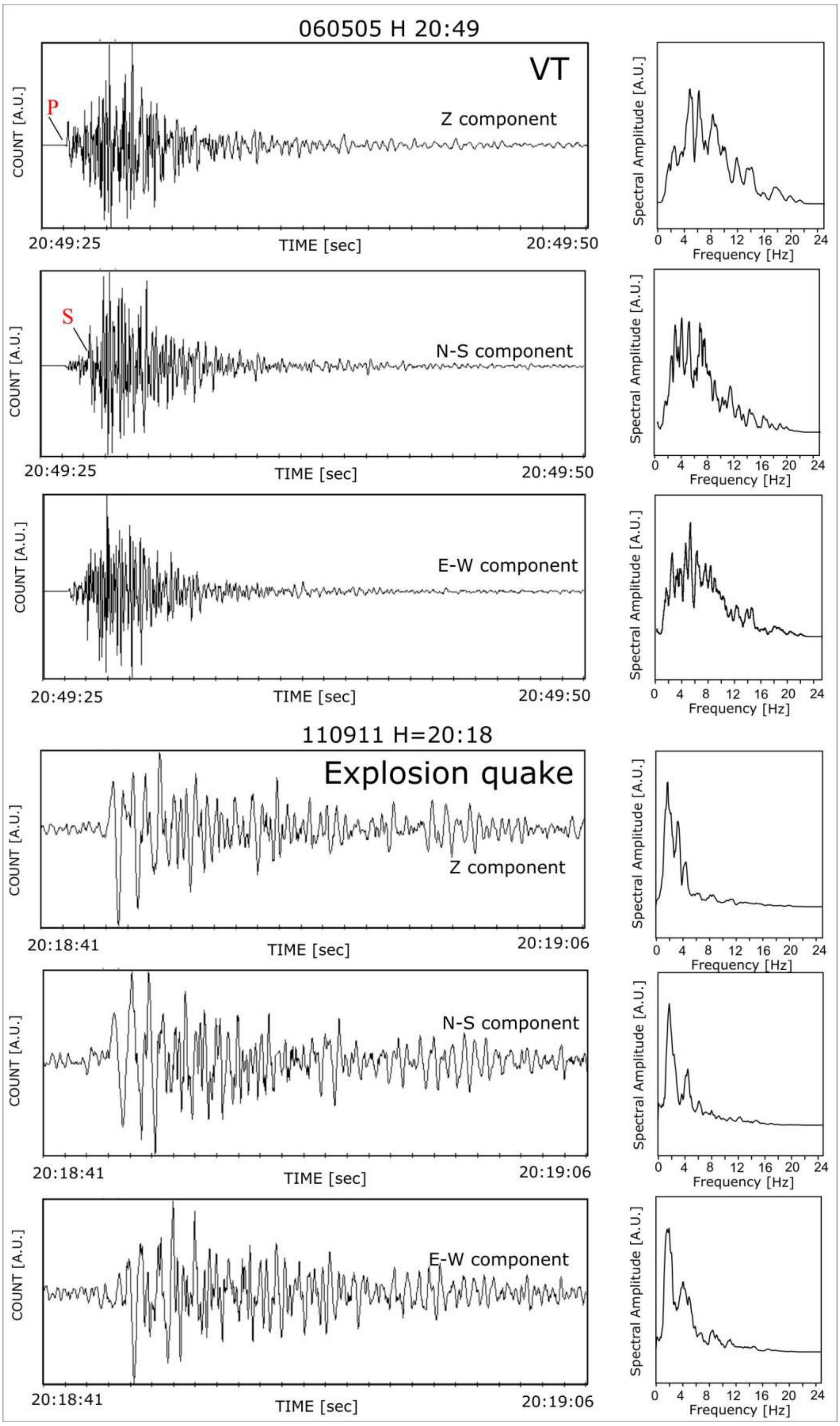
060505 H 20:49
VT
P
Z component
COUNT [A.U.]
20:49:25
TIME [sec]
20:49:50
Spectral Amplitude [A.U.]
Frequency [Hz]
S
N-S component
E-W component
110911 H=20:18
Explosion quake
20:18:41
20:19:06
0 4 8 12 16 20 24

Fig. 3

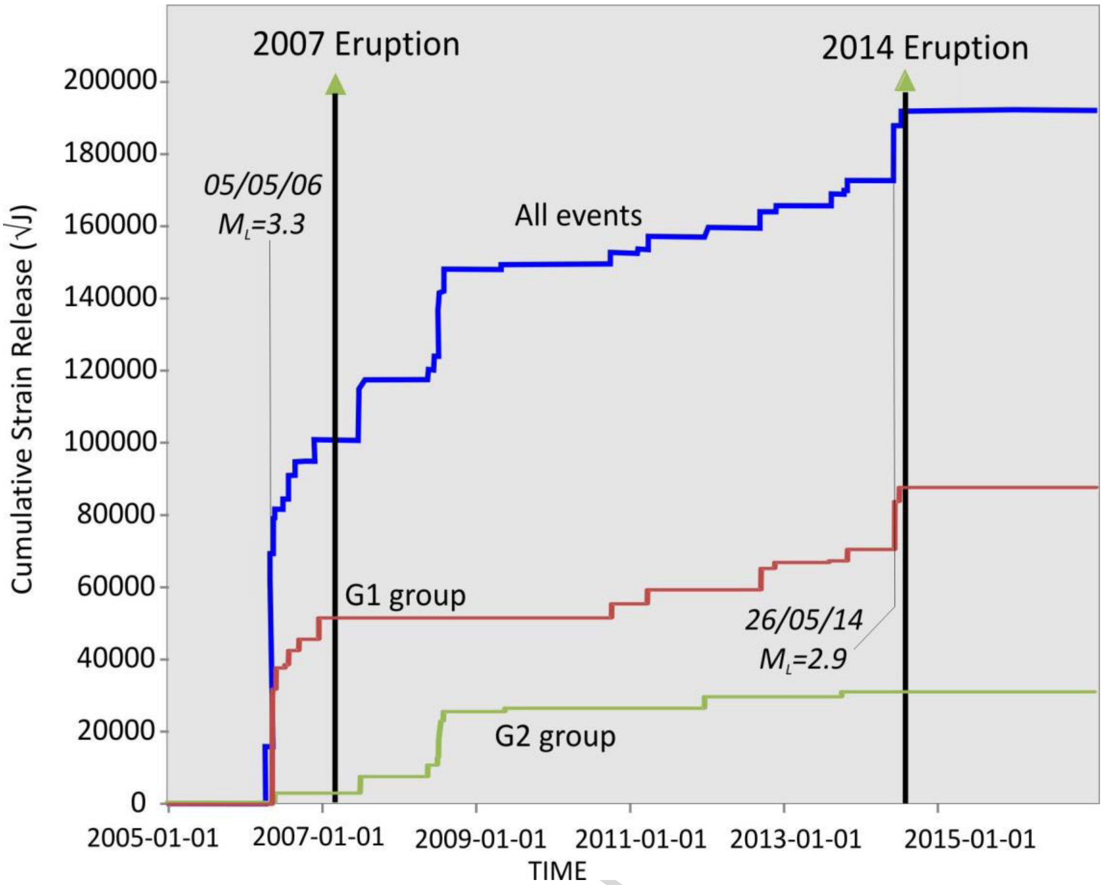
2007 Eruption
2014 Eruption
200000
180000
160000
140000
120000
100000
80000
60000
40000
20000
0
Cumulative Strain Release (√J)
05/05/06
M_L=3.3
All events
G1 group
26/05/14
M_L=2.9
G2 group
2005-01-01
2007-01-01
2009-01-01
2011-01-01
2013-01-01
2015-01-01
TIME

Fig. 4

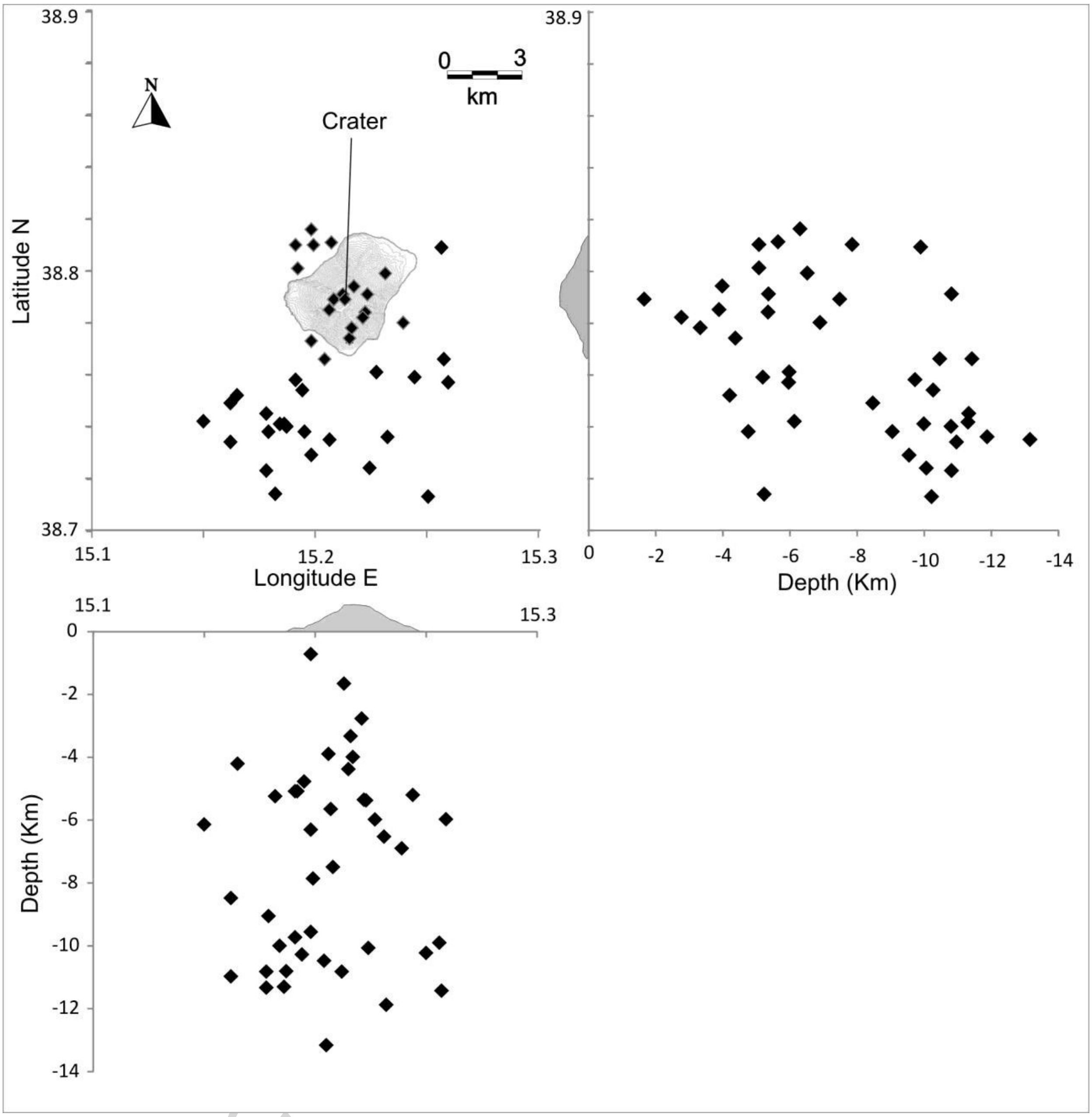
38.9
38.8
38.7
Latitude N
N
0 3
km
Crater
15.1
15.2
15.3
Longitude E
38.9
0
-2
-4
-6
-8
-10
-12
-14
Depth (Km)
15.1
15.3
0
-2
-4
-6
-8
-10
-12
-14
Depth (Km)

Fig. 5

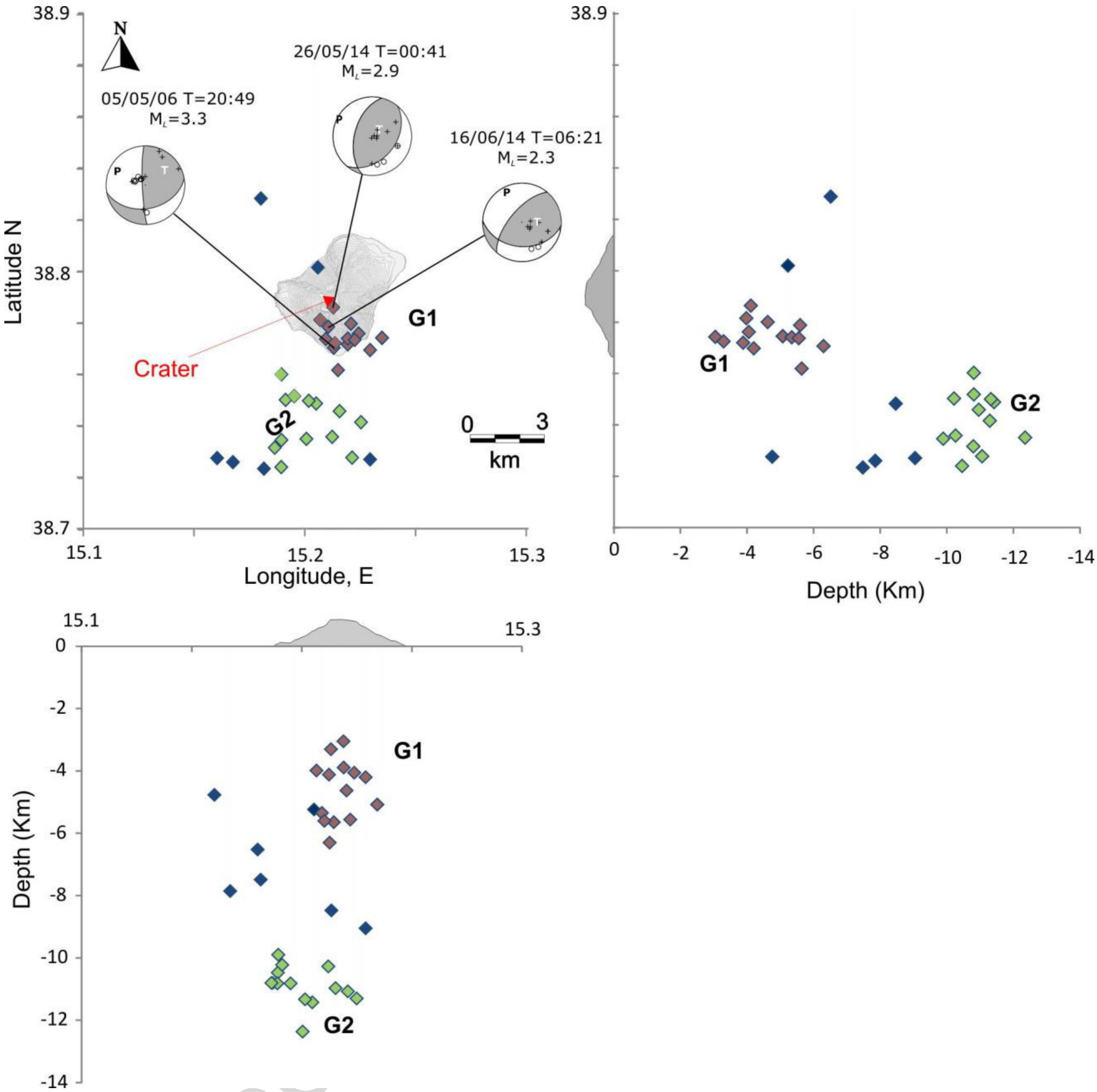

38.9
N
26/05/14 T=00:41
M_L=2.9
05/05/06 T=20:49
M_L=3.3
16/06/14 T=06:21
M_L=2.3
P
T
Latitude N
38.8
G1
Crater
G2
0
3
km
38.7
15.1
15.2
15.3
Longitude, E
38.9
G1
G2
0
-2
-4
-6
-8
-10
-12
-14
Depth (Km)
15.1
15.3
0
-2
-4
-6
-8
-10
-12
-14
Depth (Km)
G1
G2

Fig. 6

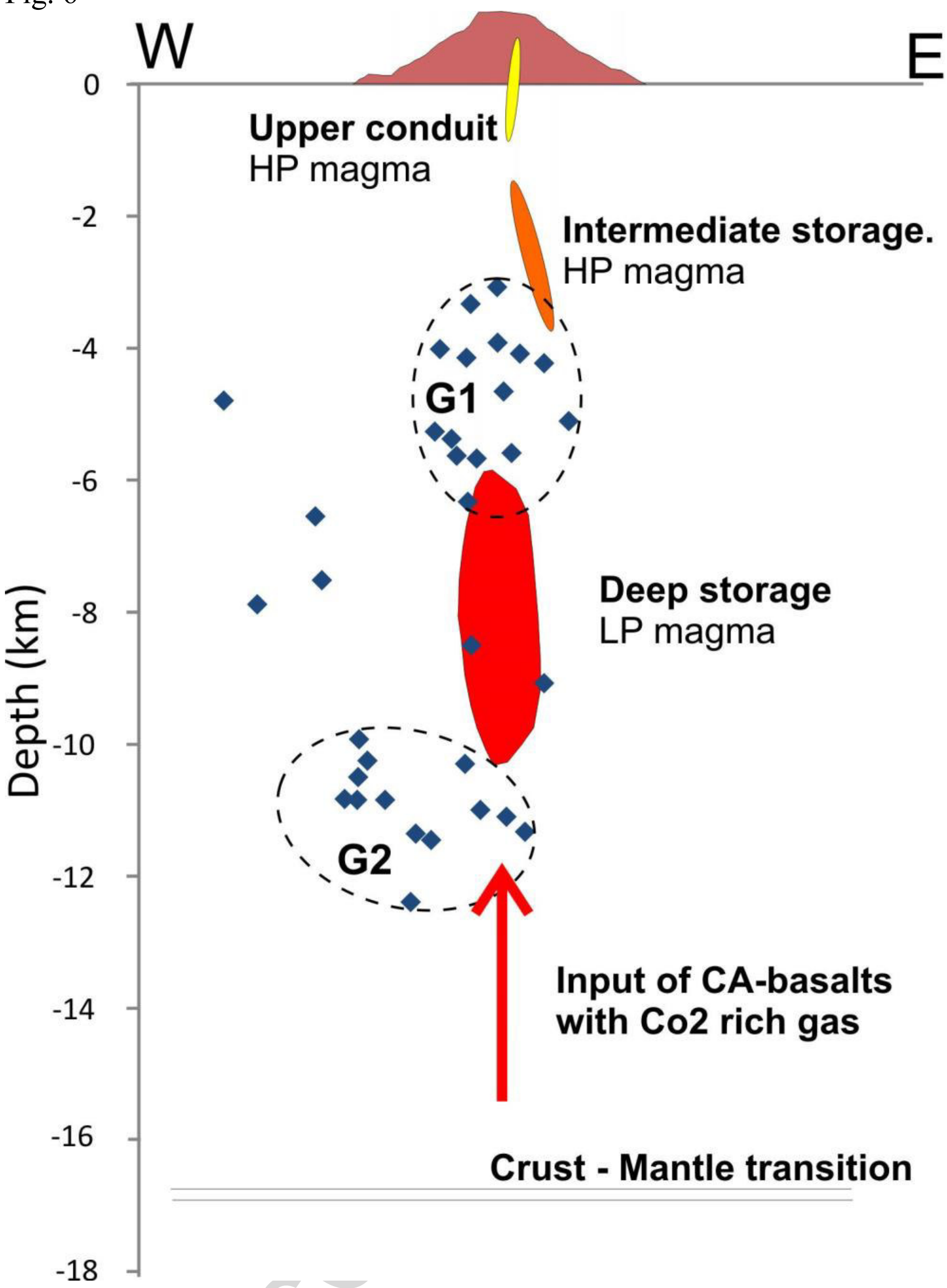

W
E
0
-2
-4
-6
-8
-10
-12
-14
-16
-18
Depth (km)
Upper conduit
HP magma
Intermediate storage.
HP magma
G1
Deep storage
LP magma
G2
Input of CA-basalts
with Co2 rich gas
Crust - Mantle transition

Highlights

We focused on Stromboli VT seismicity from 2005 to 2016;

We applied the double-difference approach to improve their locations;

We evidenced two main seismogenic sectors (G1 and G2);

Occurrence of seismic events belonging to G1 volume seems to precede the 2007 and 2014 effusive eruptions;

We suggest that faulting episodes occur as a response to local stress linked to the pressurization of the magmatic system caused by magma ascent;